Chapter 4.

Targeting a single mismatched minor histocompatibility antigen with tumor-restricted expression eradicates human solid tumors

Targeting a single mismatched minor histocompatibility antigen with tumor-restricted expression eradicates human solid tumors.

Lothar Hambach, MD[1], Marcel Vermeij[2], Andreas Buser, MD[1], Zohara Aghai[1], Theo van der Kwast, MD, PhD[2], Els Goulmy, PhD[1]
[1]Department of Immunohematology and Blood Transfusion, Leiden University Medical Center, [2]Department of Pathology, Erasmus Medical Center, Rotterdam

Regressions of metastatic solid tumors after allogeneic human leukocyte antigen (HLA)-matched stem-cell transplantation (SCT) are often associated with detrimental graft-versus-host-disease (GvHD). The graft-versus-host reaction of the HLA-matched donor is mainly directed against the multiple mismatched minor histocompatibility antigens (mHags) of the patient. mHags are strong HLA-restricted allo-antigens with differential tissue distribution. Ubiquitously expressed mHags are the prime in situ targets of GvHD. The mHag HA-1 is hematopoiesis-restricted, but displays additionally an aberrant expression on solid tumors. Thus, HA-1 might be an excellent target to boost the anti-solid tumor effect of allogeneic SCT without inducing severe GvHD. Here, we show that cytotoxic T-lymphocytes (CTLs) solely targeting the human mHag HA-1 are capable of eradicating three-dimensional human solid tumors in a highly mHag specific manner in vitro, accompanied by interferon-gamma release. In vivo, HA-1 specific CTLs distribute systemically and prevent human breast cancer metastases in immunodeficient mice. Moreover, HA-1 specific CTLs infiltrate and inhibit the progression of fully established metastases. Our study provides the first proof for the efficacy of a clinically applicable concept to exploit single mismatched mHags with hematopoiesis- and solid tumor-restricted expression for boosting the anti-solid tumor effect of allogeneic SCT.

INTRODUCTION

Allogeneic human leukocyte antigen (HLA)-matched stem cell transplantation (SCT) is an established curative treatment for hematopoietic malignancies and an investigative immunotherapeutic approach for solid tumors. Initial trials of allogeneic SCT for advanced breast and renal cell (RCC) cancer showed encouraging results with regressions of widespread metastatic lesions. Some of these clinical responses were durable for more than 4 years [1-6]. Particularly in RCC, a disease hardly responding to chemotherapy, tumor regressions after allogeneic SCT were attributed to an immune-mediated graft-versus-tumor (GvT) effect. However, broad application of allogeneic SCT in solid tumor therapy remained limited due to the risk of severe graft-versus-host disease (GvHD) mostly associated with the GvT effects [1-6]. The major challenge for further improvements of SC based allogeneic immunotherapy of solid tumors is therefore boosting specifically the GvT effect but not the GvHD immune reactivity.

The precise effector mechanisms of the GvT effect after HLA-matched allogeneic SCT are still unknown. The close association of clinical responses with GvHD suggests that the GvT effect is largely mediated by alloreactive T-cells recognizing minor histocompatibility antigens (mHags) expressed on normal and malignant cells [7]. mHags are highly immunogenic polymorphic peptides presented in the context of HLA-molecules. Despite HLA-matching of donor and patient, mHag incompatibilities remain and result in strong donor T-cell responses against mHag alleles absent in the SC donor but present in the patient [8]. Due to the “allo-ness” of mHags, mHag specific immune responses are not blunted by self-

tolerance [7]. Thereby, allogeneic SCT overcomes a major limitation of the commonly used cancer immunotherapies targeting autologous "tumor-associated antigens" (TAAs), where breaking self-tolerance remains an unsolved problem [9]. The key observation indicating that GvT effects can be separated from GvHD in man was the finding that mHags display a differential tissue distribution. mHags are derived from genes that are either ubiquitously expressed or have a tissue-restricted expression [10]. We showed earlier, that the ubiquitously expressed mHags are the prime in situ targets of GvHD [11]. Some hematopoiesis-restricted mHags are aberrantly expressed on solid tumor cells (so called "tumor mHags"). The hematopoiesis-restricted mHag HA-1 is expressed on a broad spectrum of primary solid tumors, but not on normal non-hematopoietic tissue [12,13]. Moreover, HA-1 specific cytotoxic T-lymphocytes (HA-1 CTLs) functionally recognize HA-1 on solid tumor cell lines in vitro [12]. Another known tumor mHag with HA-1 like characteristics is BCL2A1 [14]. After HLA-matched allogeneic SCT, the patient's hematopoietic system is gradually replaced by the donor hematopoiesis, which is negative for the patient's hematopoiesis- and solid tumor restricted tumor mHags. Thus, solid tumor cells remain the only relevant patient's tumor $mHag^+$ cells in the body, allowing highly selective targeting of cancer with tumor mHag CTLs.

Consequently, we suggested selective enhancement of the donor T-cell response against a single mismatched tumor mHag (such as HA-1) to boost the GvT effect with low risk of GvHD [7]. The goal of our study was to answer two core questions of our allo-immunotherapeutic concept. Firstly, are CTLs directed at a single tumor mHag capable of eradicating human three-dimensional (3D) human tumors in a mHag specific manner? Secondly, are CTLs solely targeting a single tumor mHag effective against human solid tumors in vivo? To answer these questions, we performed a detailed analysis of the efficacy of human HA-1 CTLs against human microtumors and explanted macroscopic tumors in vitro and against human macroscopic tumors and cancer metastases in translational animal models in vivo. We provide the first proof for the efficacy of the concept to eliminate cancer metastases by solely targeting mismatched tumor mHags.

MATERIALS AND METHODS

Human cancer cell lines

The cancer cell lines MCF-7 and MDA-MB-231 (American Type Culture Collection, Rockville, USA), 518A2 (kindly provided by Dr. P. Schrier, Leiden University Medical Center, The Netherlands) and BB65-RCC (kindly provided by Dr. B. Van den Eynde, Ludwig Institute for Cancer Research, Brussels, Belgium) were genomically typed for the mHags HA-1 and H-Y by allele specific PCR [15] and analyzed for HA-1 mRNA expression as described [12]. Tumor cell lines were designated "HA-1^{+}", if positive for the immunogenic HA-1^{H} allele and for HA-1 mRNA.

Generation and culturing of HA-1 and H-Y specific CTLs

The HA-1 CTL clones 1.7 and 2.12 were generated from PBMCs of HLA-$A2^{+}$/HA-1^{RR} healthy donors as described [16]. Approval was obtained from the Leiden University Medical Center review board and informed consent was provided according to the Declaration of Helsinki. The HA-1 CTL clone 3HA15 and H-Y CTL clone 21-17 were isolated from patients after allogeneic SCT [10,17].

Determination of cytotoxicity and IFN-γ release

Tumor cell killing by CTLs was tested in a standard 4-hr ^{51}Cr release assay as described [16]. IFN-γ concentrations were determined with the Pelikline ELISA kit (CLB, Amsterdam, The Netherlands). Detection limit was 2 pg/mL.

Microtumor model

Microtumors in collagen matrix were generated according to a modified protocol [18](L.H., E.G., manuscript in preparation). In brief, $6x10^4$ tumor cells in 0.6 µl 3.65 mg/ml rat tail collagen type I (BD Biosciences Europe, Erembodegem, Belgium) were embedded between two layers of 50 µl collagen (base layer: 1.75 mg/ml, top layer: 1.31 mg/ml) and covered with 100 µl of 20% human serum (HS) in IMDM (Invitrogen Life Technologies, Breda, The Netherlands). After 1 day, medium was replaced by 100 µl 20% HS in IMDM containing 240 IU/ml IL-2 (Chiron, Amsterdam, The Netherlands) and which was supplemented with CTLs or not. Microtumor growth was photographically documented with an inverted microscope (Axiovert 25, Zeiss, Jena, Germany). Two-dimensional microtumor area π*r1*r2 was calculated after determination of the 2 maximal orthogonal microtumor radii r1 and r2 (AxioVision 40 LE Version 4.5, Sliedrecht, The Netherlands). For histological analysis, microtumors in collagen type I were fixed with 4% formalin for 24h at 4ºC and embedded in paraffin as described in detail (manuscript in preparation). H&E stainings were performed on 4 µm serial sections. Histological analysis was performed by two independent pathologists.

Mouse models

Mice. 7-11 weeks old female NOD/scid mice (Charles River, France) were used. Experiments were performed after approval of the ethical committee of the Leiden University Medical Center.

Model of s.c. macrotumors. Mice were s.c. inoculated with $5x10^6$ MDA-MB 231 cells in 200 µL IMDM with 1% FCS (Invitrogen Life Technologies). Human CTLs were quantified in peripheral blood samples and in organ and bone marrow suspensions by flowcytometry as described [19].

Model of pulmonary microtumors. Mice were inoculated i.v. in a lateral tail vein with $5x10^5$ or $7.5x10^5$ MDA-MB 231 cells in 200 µL 1% FCS in IMDM and sacrificed on day 40 or day 50, respectively. Lungs were inflated with 4% formalin via the trachea and fixed over night at 4°C. Tumor nodules on the lung surface were quantified with a stereo dissecting microscope (Leica MZ 7.5, Rijswijk, The Netherlands)**.** 4 µm serial sections were cut from paraffin-embedded right lung lobes. Intrapulmonal microtumors were counted after staining with anti-human cytokeratin antibodies.

Adoptive CTL transfer protocol. Mice were treated by i.v. administration of $3x10^7$ CTLs in 200 µL 1% FCS in IMDM or with PBS as control as described [20]. All mice received $2x10^4$ IU IL-2 intraperitoneally daily for 3 weeks.

Ex vivo tumor T cell infiltration assay

S.c. established tumors were explanted from untreated NOD/scid mice. 3 mm diameter punch biopsies were sectioned horizontally at a height of 2-3 mm, placed on a transwell insert with 0.4 µm pore size (BD Biosciences, Franklin Lakes, USA) of a 24 well plate and demobilized with 100 µl rat tail collagen type I. 600 µl 10% HS in IMDM with 120 IU IL-2 and $1x10^6$ HA-1 CTLs were added to the insert and 1 ml 10% HS in IMDM with 120 IU IL-2 were added to the well. Medium was replaced every day. On day 3 after addition of CTLs, tumors in collagen type I were fixed with 4% formalin and 24h later embedded in paraffin.

Immunohistochemistry

Sections were stained with anti-human CD8 antibody (clone 4B11, dilution 1/20, Novocastra, UK) or pankeratin Ab-1 antibody (clone AE1/AE3, dilution 1/160, Labvision, Duiven, The Netherlands). Detection was performed with DAKO Envision Peroxidase/DAB kit (Dako, Heverlee, The Netherlands). Sections were counterstained with Mayer hematoxylin.

Statistical Analysis

Different groups of mice were pair-wise compared by a Mann-Whitney-U test using SPSS 14.0 (SPSS Inc., Chicago, IL, USA). A p-value < 0.05 was considered statistically significant.

RESULTS

HA-1 CTLs kill HA-1$^+$ solid tumor cells in vitro

In order to answer the question whether CTLs directed a single tumor mHag are capable to clear solid tumors in a mHag specific manner, we selected a panel of solid tumor cell lines with differential molecular expression of the tumor mHag HA-1 and the ubiquitously expressed mHag H-Y for the subsequent experiments (Supplemental Table S1, Supplemental Figure S1A). HA-1 and H-Y served as mutual controls for the mHag specificity of HA-1 or H-Y CTLs. Since recognition of the mHags HA-1 and H-Y by CTLs is HLA-A2 restricted, all selected tumor cell lines were HLA-A2$^+$. The expression levels of HLA-A2 differed between the tumor cell lines, while the expression of cell adherence molecules was comparable (Supplemental Figure S1B). MHag specific cytotoxicity of the previously established HA-1 CTL clones 1.7, 2.12 and 3HA15 and the H-Y CTL clone 21-17 was tested in a standard 4h ^{51}Cr-release assay. The HA-1 CTL clones lysed only HA-1$^+$ target cells, including the RCC cell line BB65-RCC and the breast cancer cell line MDA-MB-231 (Figure 1 A-C). The H-Y CTL clone lysed only H-Y$^+$ target cells, including the RCC cell line BB65-RCC and the melanoma cell line 518A2 (Figure 1 A, B, E). The avidity of the different HA-1 CTLs clones for their target cells was comparable (Supplemental Figure S2A). All HA-1 CTL clones used in this study displayed a marker profile consistent with a terminally differentiated effector memory T-cell phenotype (CD3+, CD8+, CD45RA-, CD62L-, CD27-, CD28-) (Supplemental Figure S2B).

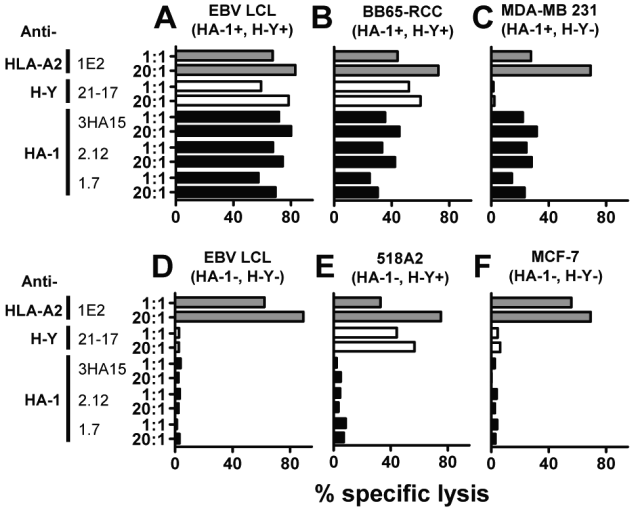

Figure 1. HA-1 CTLs lyse tumor cells in vitro. The in vitro killing efficacy of CTLs was determined in a Chromium^{51} release assay. All target cells are HLA-A2$^+$. The allo HLA-A2 CTL clone lyses all target cells, the HA-1 CTL clones lyse only HA-1$^+$ target cells and the H-Y CTL clone lyses only H-Y$^+$ target cells; x-axis, mean percent specific lysis (2 measurements per condition); y-axis, CTL clones each in 2 different effector to target ratios. EBV LCL: Epstein–Barr virus-/lymphoid cell line.

HA-1 CTLs eradicate human 3D microtumors in vitro

To assess to the efficacy and mHag specificity of particularly HA-1 CTLs against human microtumors in vitro, we developed an in vitro model allowing real-time assessment of immunotherapeutic effects on individual human 3D microtumors (L.H., E.G., manuscript in preparation). Tumor cell agglomerates were embedded in a collagen scaffold resulting in progressively growing tumors. Microtumors showed a multilayer morphology on day 3 (data not shown) and 7 (Figure 2E-H) mimicking clinical cancers of the same entities as the tumors from which the tumor cell lines were derived (Supplemental Table S1), both histopathologically (Figure 2A-D) and immunohistochemically (L.H., E.G., manuscript in preparation).

We applied these microtumors to investigate mHag CTL-mediated tumor clearance, CTL-tumor infiltration and cytokine release within one model. Microtumors were generated on day 0 and medium alone, HA-1 or H-Y CTLs were added on day 1. CTLs required 2-3 days to reach the microtumors as determined by light microscopy. On day 7, all HLA-$A2^+$ microtumors were destroyed by the allo-HLA-A2 CTL clone 1E2 (data not shown). All three HA-1 CTLs clones 1.7, 2.12 and 3HA15 eliminated at an effector to target ratio of 15:1 the HA-1^+ microtumors BB65-RCC (Figure 2E) and MDA-MB 231 (Figure 2F), while leaving the HA-1^- microtumors 518A2 (Figure 2G) and MCF-7 (Figure 2H) intact. The H-Y CTL clone 21-17 destroyed only the H-Y^+ microtumors BB65-RCC (Figure 2E) and 518A2 (Figure 2G) without affecting growth of the H-Y^- microtumors MDA-MB 231 (Figure 2F) and MCF-7 (Figure 2H). Immunohistochemistry on day 3 revealed that all HA-1 and H-Y CTL clones infiltrate all microtumors.

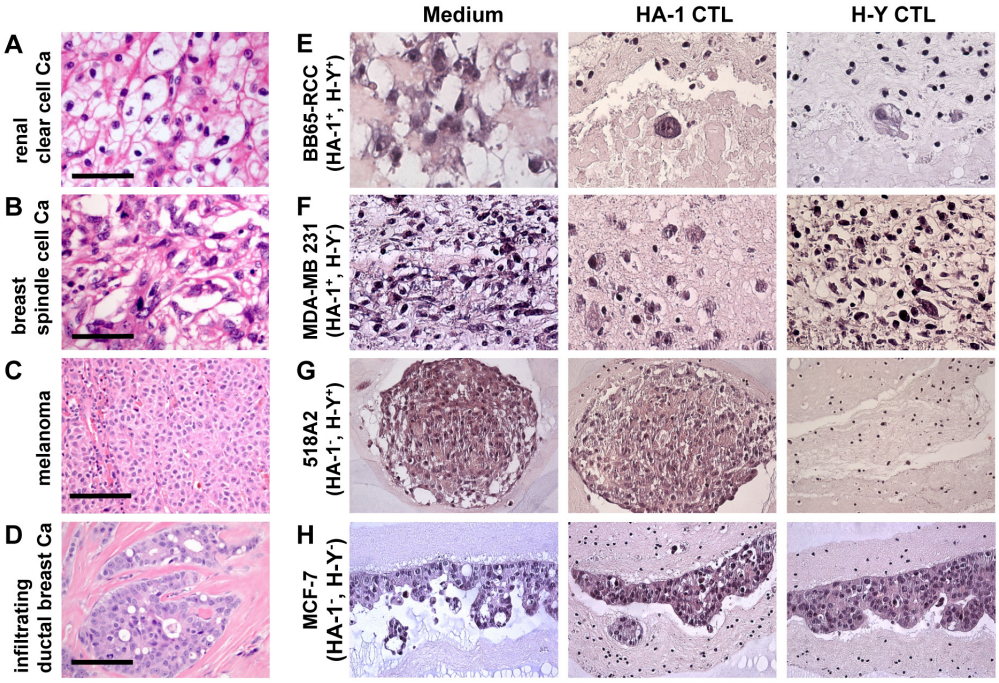

Figure 2. HA-1 CTLs eradicate 3D microtumors mimicking primary tumors. (A-D, E-H medium controls) H&E stainings reveal that microtumors (E-H medium controls) closely resemble the histologies of the corresponding primary tumors (A-D). BB65-RCC microtumors (E) show clear cells similar to a primary intermediately differentiated renal cell carcinoma (A). MDA-MB 231 microtumors (F) contain spindle formed cells without orientation similar to a primary spindle cell carcinoma of the breast (B). 518A2 microtumors (G) show sheets of cells similar to a primary melanoma (C). MCF-7 microtumors (H) show acinus like structures similar to a primary intraductal carcinoma (D). (E-H) HA-1 and H-Y CTLs destroy microtumors in a strictly mHag specific manner, resulting in strongly reduced cellularity and cell debris. Bar: upper 2 rows 100 µm, lower 2 rows 50 µm.

However, the extent of microtumor infiltration by mHag CTLs was dependent of the expression of the relevant mHag by the microtumors (Figure 3A-B, Supplemental Figure S3). Longitudinal assessment of the tumor size on day 3 and 7 revealed that all mHag CTL clones inhibited tumor growth in a mHag specific and CTL dose-dependent manner (Figure 3C). Prolongation of the observation period from 7 to

14 days in the mHag specifically treated groups showed no progression of microtumors (Supplemental Figure S4A). Anti-tumor effects of HA-1 and H-Y CTLs were associated with mHag specific release of interferon-γ (IFN-γ), which was maximal on day 3 and subsequently declined (Figure 3D). These results demonstrate that HA-1 CTLs can eradicate human solid tumors in a highly mHag specific manner and that H-Y CTLs are equally effective.

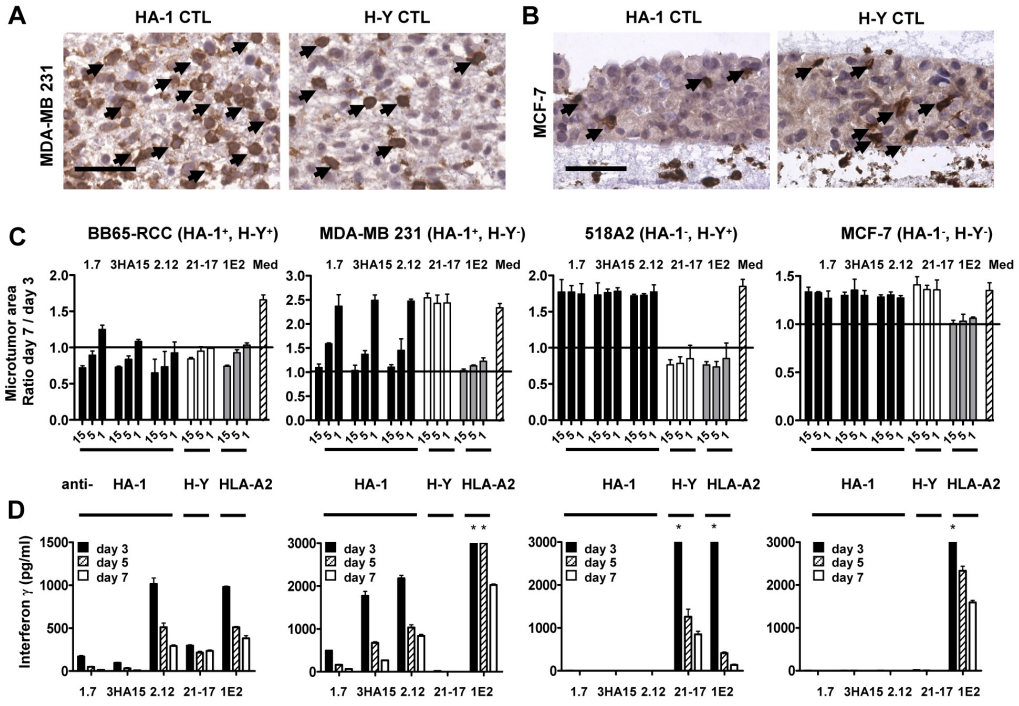

Figure 3. HA-1 CTLs infiltrate 3D microtumors, inhibit tumor growth and release IFN-γ. (A,B) CD8 staining of MDA-MB 231 (A) and MCF-7 (B) microtumors after 3 days of co-incubation with HA-1 or H-Y CTLs. Arrowheads indicate CD8+ CTLs; bar, 50 µm. (C) Microtumor growth inhibition after addition of the anti-HA-1, H-Y or HLA-A2 CTLs. x-axis, CTL clones each in 3 different effector–target ratios (15:1, 5:1, 1:1) or medium; y-axis, ratio between the microtumor areas in photographs of day 7 and day 3. Bars correspond to mean +/- S.E.M. (data are pooled from 3 independent experiments resulting in median 3 (range 2-8) microtumors per condition). (D) IFN-γ in the supernatant of microtumors after addition of anti- HA-1, H-Y CTL and HLA-A2 CTLs in an effector to target ratio of 15:1. x-axis, day 3, 5 and 7 after addition of different CTL clones; y-axis, IFN-γ in the supernatant. Bars correspond to mean +/- S.E.M. (4 measurements per sample). Star indicates off-scale measurement.

In vivo distribution of HA-1 CTLs

Due to their restricted tissue expression, only tumor mHags (such as HA-1) are suitable as targets for mHag specific immunotherapy of solid tumors after allogeneic SCT. In order to investigate whether CTLs directed at a single tumor mHag HA-1 are capable to eradicate solid tumors in vivo, we designed translational animal models. In these models, human solid tumors were engrafted in immunodeficient non-obese diabetic/severe combined immunodeficiency (NOD/scid) mice and subsequently treated with human mHag CTLs. Based on its aggressive localized and metastatic growth [21], we selected the HA-1^{+}/H-Y^{-} breast cancer cell line MDA-MB 231 as tumor target in our in vivo experiments. Subcutaneous

(s.c.) macrotumors were established in NOD/scid mice by s.c. injection of $5x10^6$ MDA-MB 231 cells which induced progressively growing tumors of 8-10 mm diameter on day 30 in all mice (data not shown). Aiming at treatment of human s.c. macrotumors in NOD/scid mice, we determined survival, in vivo distribution and tumor infiltration of HA-1 CTLs. We selected for comparative adoptive CTL transfer experiments the best expandable HA-1 CTL clone 1.7 used in this study (data not shown). Mice with a tumor diameter of 6-8 mm received $30x10^6$ HA-1 CTLs intravenously (i.v.). Tracking of adoptively transferred HA-1 CTLs on day 1, 3, 7, 14 and 21 after CTL administration showed systemic distribution of human CTLs into lung, liver, spleen, bone marrow and peripheral blood (% infiltrations of the analyzed organs by HA-1 CTLs are depicted in Figure 4A; absolute numbers of HA-1 CTLs in the analyzed organs are depicted in Supplemental Figure S5). On day 1 after CTL transfer, CTL infiltration was highest in the lungs, while all other organs showed infiltration at lower and comparable levels. HA-1 CTLs redistributed from the lungs on day 1 to the bone marrow on day 3 (Supplemental Figure S5). HA-1 CTL infiltration of the various organs persisted for up to 14 days after CTL administration, most pronounced in the bone marrow. No HA-1 CTLs were found in the peripheral blood beyond day 3. At none of the time-points analyzed, substantial levels of HA-1 CTLs were detected in s.c. macrotumors (Figure 4A and Supplemental Figure S5). Thus, we did not continue to perform experiments determining the in vivo efficacy of HA-1 CTLs against s.c. macrotumors.

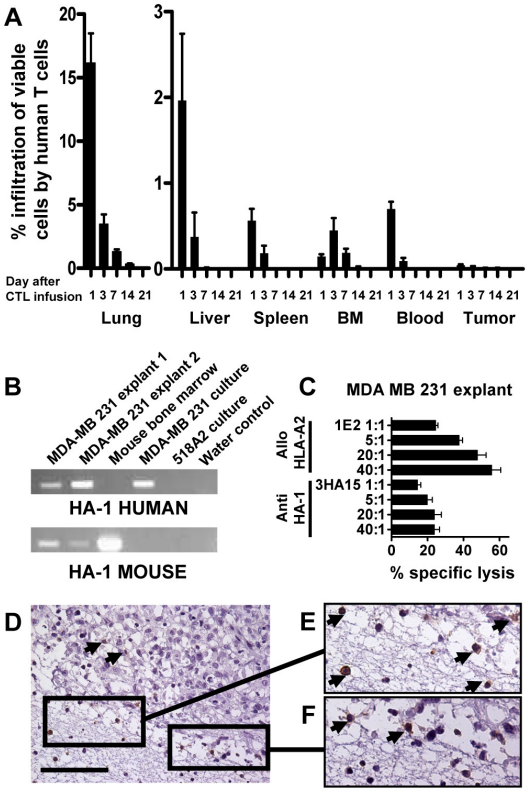

Figure 4. In vivo distribution of HA-1 CTLs and ex vivo analysis of s.c. macrotumors. (A) NOD/scid mice with s.c. MDA-MB 231 macrotumors were treated with a single dose of $30x10^6$ HA-1 CTLs (clone 1.7) i.v. HA-1 CTLs were quantified by flowcytometry in lung, liver, spleen, bone marrow, peripheral blood and the solid tumor at 1, 3, 7, 14 or 21 days after CTL transfer. Depicted are the percentage of viable human CTLs in relation to all measured viable cells in the individual tissues. Bars correspond to mean +/- S.E.M. (4 mice per measurement time point). (B) HA-1 mRNA expression in single cell suspensions of MDA-MB 231 macrotumors freshly explanted from 2 individual untreated (i.e. without HA-1 CTL infusion) NOD/scid mice, mouse bone marrow, cultured MDA-MB 231 and 518A2 cells determined with human (top row) and mouse (bottom row) HA-1 specific primers. Weak mouse HA-1 mRNA signals in the explanted tumor samples indicate contamination with mouse hematopoietic cells. (C) Single cell suspensions of MDA-MB 231 macrotumors freshly explanted from 3 individual untreated NOD/scid mice were lysed by allo HLA-A2 and HA-1 CTLs; x-axis, percent specific lysis (mean +/- S.E.M.); y-axis, CTL clones in 4 different effector–target ratios. (D-F) Biopsies of MDA-MB 231 s.c. macrotumors explanted from untreated NOD/scid mice were embedded in collagen type I matrix and co-incubated with the HA-1 CTL clones 1.7, 2.12 and 3HA15 for 3 days. Shown is a representative example of a human CD8 staining. HA-1 CTLs are only present in the surrounding collagen type I matrix and the tumor border (D-F); Arrowheads indicate $CD8^+$ CTLs; bar, 100 µm.

HA-1 CTLs hardly infiltrate HA-1$^+$ human s.c. macrotumors ex vivo

The absence of HA-1 CTLs in macrotumors led us to question HA-1 expression in s.c. macrotumors in vivo. Single cell suspensions of MDA-MB 231 macrotumors freshly explanted from untreated mice (i.e. without previous HA-1 CTL infusion) were, however, positive for HA-1 mRNA (Figure 4B) and were recognized by allo-HLA-A2 and HA-1 CTLs in a 4h ^{51}Cr-release assay (Figure 4C). Moreover, growth of microtumors generated from explanted tumor cells was equally well inhibited by HA-1 CTLs as microtumors generated from MDA-MB 231 cells without in vivo passage (Supplemental Figure S4B). Thus, MDA-MB 231 tumor cells maintain functional HLA-A2/HA-1 expression upon in vivo growth. Next, we determined whether absence of tumor infiltration by CTLs was related to the characteristic of one individual HA-1 CTL clone. Thus, we embedded 3 mm punch biopsies of MDA-MB 231 macrotumors explanted from untreated mice in collagen type I matrix and co-incubated these biopsies with 1x10^6 cells of the HA-1 CTL clones 1.7, 2.12 and 3HA15. CD8 staining on parallel sections on day 3 showed abundant presence of all HA-1 CTL clones in the collagen matrix and on the tumor border, but only very few HA-1 CTLs within the tumor (Figure 4D-F). Thus, HA-1 CTLs hardly infiltrate human s.c. macrotumors, despite in vivo maintenance of HA-1 expression.

HA-1 CTLs prevent and inhibit the progression of human lung metastases in vivo

Subsequently, we investigated whether the direct HA-1 CTL - human tumor cell in vivo interaction is effective in preventing pulmonary metastasis. I.v. injection of HA-1$^+$/H-Y$^-$ MDA-MB 231 tumor cells in the lateral tail vein on day 0 resulted in median 37 (range 4-80) and 159 (range 111-399) pleural tumor nodules on the intact lungs after 40 and 50 days (representative examples depicted in Figure 5A), respectively. Cytokeratin staining on parallel sections revealed microtumors in the pulmonary interstitium of which some were subpleurally localized (Figure 5B). Quantification of the microtumors revealed median 13 (range 2.3-40.1) and 25 (range 19.2-48.1) microtumors per section after 40 and 50 days, respectively. No metastases in other organs (liver, spleen, bone marrow, kidneys) were found (data not shown). Three days after i.v. inoculation of MDA-MB 231 tumor cells, when disseminated tumor cells were already detectable (Figure 5E), a single dose of 30x10^6 HA-1 CTLs, H-Y CTLs or PBS as control were administered i.v. HA-1 CTLs and H-Y CTLs showed comparable kinetics in the peripheral blood and were undetectable after 3 days upon CTL administration (Supplemental Figure S6). Mice having received the control H-Y CTLs or PBS showed on day 40 and 50 no significant difference in the number of pleural tumor nodules ($p=0.468$, $p=0.754$) or intrapulmonal microtumors ($p=0.386$, $p=0.602$), which excluded unspecific effects due to the procedure of CTL infusion (Figure 5C-D). In contrast, mice injected with the HA-1 CTL clone showed pleural tumor nodules in none of the mice on day 40 (difference in number of pleural tumor nodules compared to the PBS and H-Y CTL treated groups: $p=0.014$ and $p=0.014$, respectively) or in only 1/6 mice on day 50 ($p=0.004$ and $p=0.007$, respectively) (Figure 5C). Intrapulmonal microtumors after treatment with HA-1 CTLs were detectable in 3/4 mice on day 40 (difference in number of intrapulmonal microtumors compared to the PBS and H-Y CTL treated groups: $p=0.021$ and $p=0.021$, respectively) or in 2/6 mice on day 50 ($p=0.005$ and $p=0.009$, respectively) (Figure 5D). Thus, HA-1 CTLs eradicate disseminated tumor cells and, thereby, prevent human metastases in NOD/scid mice. Subsequently, we tested the anti-tumor efficacy of HA-1 CTLs against fully established pulmonary metastases. NOD/scid mice engrafted with MDA-MB 231 tumor cells i.v. were injected with a single dose of 30x10^6 HA-1 CTLs or H-Y CTLs or PBS as control i.v. on day 40. On day 50, mice were sacrificed. Immunohistochemistry showed infiltration of pulmonary

metastases by HA-1 CTLs (Figure 5F). Quantification of pulmonary tumors revealed no significant difference in the number of pleural tumor nodules (p=0.522) or intrapulmonal microtumors (p=0.631) in the control groups (PBS and H-Y CTLs). In contrast, mice injected with the HA-1 CTL clone showed significantly less pleural (difference in number of tumor nodules compared to the PBS and H-Y CTL treated groups: p=0.005 and p=0.004, respectively) (Figure 5C) and intrapulmonal tumor nodules (p=0.005 and p=0.009, respectively) (Figure 5D). Thus, HA-1 CTLs inhibit the progression of fully established human cancer metastases in NOD/scid mice.

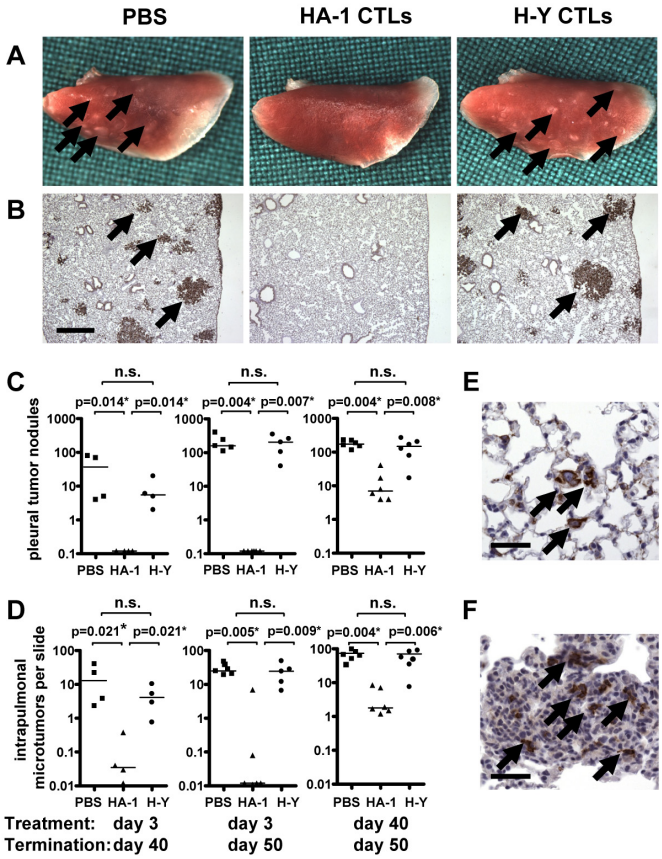

Figure 5. HA-1 CTLs prevent and inhibit the progression of pulmonary metastases. (A-F) NOD/scid mice received human HA-1^{+}/H-Y^{-} MDA-MB 231 breast cancer cells i.v. on day 0 and were treated with PBS or 30x10^{6} HA-1 or H-Y CTLs i.v. (A,B) Depicted are representative examples of lungs of mice that had been treated with PBS (left), the HA-1 CTL clone 1.7 (middle) and the H-Y CTL clone 21-17 (right) on day 3 and sacrificed on day 50. Larger pleural tumor nodules are macroscopically visible (A). Cytokeratin staining shows microtumors in the pulmonary interstitium of which some were subpleurally localized; bar, 500 µm (B). Arrowheads indicate tumors. (C,D) Quantification of pulmonary tumors of mice that had been treated on day 3 and sacrificed on day 40 (left graphs; 4 mice per group, 5x10^{5} tumor cells per mouse) or on day 50 (middle graphs, 5-6 mice per group, 7.5x10^{5} tumor cells per mouse); quantification of pulmonary tumors of mice that had been treated on day 40 and sacrificed on day 50 (right graphs, 6 mice per group, 7.5x10^{5} tumor cells per mouse). x-axis, treatment with PBS, HA-1 or H-Y CTLs; y-axis, number of pleural tumor nodules visible on the intact lungs (C) or number of intrapulmonal microtumors per parallel section (D). Numbers of lung tumors were pair-wise compared in different groups of mice by Mann-Whitney-U test. N.s.: not significant. (E) Cytokeratin staining of single tumor cells in the lungs of mice 3 days after i.v. administration of MDA-MB 231 tumor cells; bar, 50 µm. (F) CD8 staining of a pulmonary metastasis of mice that had been treated on day 40 with HA-1 CTLs and sacrificed on day 50. Arrowheads indicate CD8+ CTLs; bar, 50 µm.

DISCUSSION

Our study is the first to show the potency and mHag specificity of human mHag HA-1 CTLs to destroy human 3D microtumors that closely resemble clinical micrometastases and avascular tumor stages. Although mHag HA-1 expression on single tumor cells has been described [12,13,22], its clinically relevant functional expression on 3D tumors was as yet unknown. Tumor eradication by HA-1 CTLs points towards crucial differences in the functional expression of the mHag HA-1 on solid tumors compared to tumor associated antigens (TAAs), which are commonly used as targets for cancer immunotherapy. While 3D tumor growth results in loss of TAA presentation [23,24] and in "multicellular apoptosis resistance" [25,26] within 24h, the functional mHag HA-1 expression and tumor susceptibility to mHag CTL lysis were not hampered by the 3D tumor growth in our study. Interestingly, complete microtumor eradication has not been shown for human TAA specific CTLs, to the best of our knowledge. A possible explanation might be the frequently lacking TAA expression in a considerable proportion of cancer cells in clinical tumors, as shown for melanocyte differentiation (e.g. MelanA/MART-1 or gp100) [27] and for cancer testis antigens (e.g. MAGE–1 or NY-ESO-1) [28,29]. Also experimental 518A2 melanomas used in our study were only heterogeneously positive for MelanA (data not shown). The complete eradication of microtumors by HA-1 CTLs provides a first indication that HA-1 is expressed on the vast majority of tumor cells in our model. Nevertheless, it needs to be considered that primary tumors may have a more complex hierarchy of cancer stem cells and progeny than reflected by tumor cell lines in our model. Thus, further studies using HA-1 specific antibodies or probes for mRNA in situ hybridization are required to exactly determine the homogeneity of HA-1 expression, particularly in clinical tumors. Overall, the capability of HA-1 CTLs to infiltrate microtumors, to inhibit tumor growth and, ultimately, to eradicate human microtumors in a highly mHag specific manner, qualifies HA-1 as powerful allogeneic target on solid tumors.

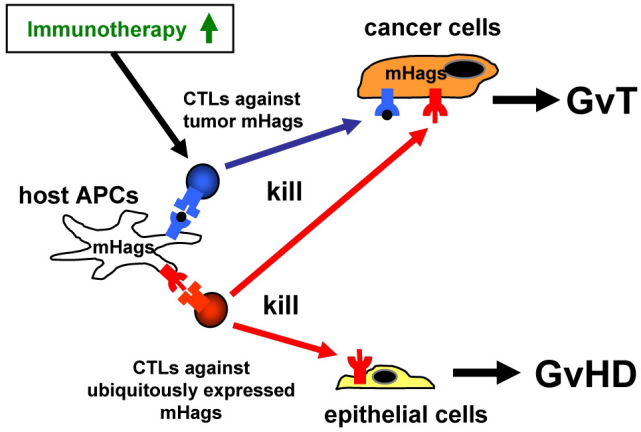

Figure 6. Targeting solely mismatched tumor mHags boosts the GvT effect. HLA-matched patients and donors remain mismatched for multiple mHags. According to our working hypothesis, host-derived antigen presenting cells (APCs) persisting after allogeneic SCT induce an anti-host response of donor T-cells. Based on the mHag tissue distribution, the anti-host response is dissected into a branch mediating GvT effects only and a branch mediating both GvT effects and GvHD. Our findings indicate that immunotherapy targeting mismatched tumor mHags only is sufficient to boost the GvT effect.

However, after HLA-matched allogeneic SCT, the tumor mHag HA-1 is only one of many mismatched mHags driving the GvH response. Accordingly, also CTLs directed against the GvHD target antigen H-Y were highly effective in eradicating human solid tumors in our study in vitro. In fact, both mHag CTLs against tumor mHags (HA-1) and against ubiquitously expressed mHags (HA-3 and HA-8) are detectable

in solid tumor patients responding to allogeneic SCT [22]. The individual contribution of CTLs against tumor mHags and CTLs against ubiquitously expressed mHags to the GvT effect is unknown. However, the high efficacy of HA-1 CTLs in our study in vitro indicates that solely targeting tumor mHags might be sufficient to boost the anti-solid tumor response in vivo (Figure 6).

Accordingly, adoptive transfer of a single dose of HA-1 CTLs was highly effective in eradicating disseminated tumor cells and, thereby, preventing pulmonary breast cancer metastases in our study in vivo. Although eradication of murine tumors by targeting a ubiquitously expressed murine mHag was recently demonstrated by Perreault and co-workers [30], we here show for the first time the in vivo anti-tumor efficacy of CTLs directed against a human tumor-restricted and, thus, clinically relevant mHag. Several factors might have contributed to the high in vivo efficacy of HA-1 CTLs. Firstly, adoptively transferred CTLs temporarily accumulated in the lungs on day 1. Thus, administered CTLs passively encounter lung metastases via the pulmonary circulation. Of note, the systemic distribution of HA-1 CTLs observed in the macrotumor model indicates that HA-1 CTLs have the potential to eliminate solid tumor cells at all possible sites of metastases in all organs. Secondly, the high CTL to tumor cell ratio (>40:1) has likely contributed to the anti-solid-tumor efficacy of HA-1 CTLs. This assumption is supported by the CTL dose-dependent long-term efficacy of mHag CTLs against microtumors in vitro and our previous observation that HA-1 CTLs were only effective against minimal leukemic disease in NOD/scid mice, while not against overt leukemia [20]. Finally, the direct contact of administered CTLs with the disseminated tumor cells without the need of tumor infiltration may have facilitated the anti-tumor efficacy of HA-1 CTLs in this model. However, HA-1 CTLs also inhibited the progression of pulmonary metastases fully established as 3D tumor structures. This finding is particularly relevant in cases in which complete remissions cannot be achieved by conventional treatments before HA-1 specific immunotherapy. Overall, our in vivo data demonstrate that HA-1 CTLs are therapeutically highly effective against solid tumors in minimal disease.

In contrast, s.c. macrotumors represented a limitation in our NOD/scid mouse tumor model, as in this setting hardly any tumor infiltrating HA-1 CTLs could be detected. This finding reflects conflicting data on tumor infiltration by TAA CTLs upon adoptive transfer in man. Despite indications for infiltration by TAA CTLs were found in some metastatic melanoma lesions of few evaluated patients [31-33], most metastases seemed to be spared by TAA CTLs. The reasons for low tumor infiltration by human CTLs specific for single tumor epitopes are poorly understood. In our in vivo s.c. macrotumor model, the systemic distribution of transferred CTLs suggests that HA-1 CTLs can reach the circulation of the well vascularized MDA-MB 231 tumors (data not shown). Potential difficulties for CTLs to home to tumors or to cross the xenogeneic tumor endothelium cannot be excluded by our experiments. However, we have ruled out a loss of functional HLA-A2/HA-1 target antigen expression in vivo. The fact that all three tested HA-1 CTL clones were hardly detectable in tumor biopsies upon in vitro co-incubation makes an individual characteristic of one particular CTL clone unlikely as reason for low macrotumor infiltration. The absence of human HA-1 cross-presentation by mouse stromal cells in s.c. macrotumors may lead to insufficient stimulation of CTL migration [34]. Also CTL deletion by e.g. intratumoral nutrition deprivation or “tumor counter attack” [9] need to be considered. However, our finding that in vitro microtumors and pulmonary metastases were – in contrast to s.c. macrotumors - considerably infiltrated by HA-1 CTLs might also point towards differences in the composition of the various MDA-MB 231 tumors. In fact, the compactness of the tumor histology increased from in vitro microtumors over pulmonary metastases to s.c. macrotumors (Supplemental Fig. S7A). Moreover, the higher compactness of the larger (8 mm at

explant) s.c. macrotumors compared to the smaller (<1 mm) pulmonary metastases was associated with a much higher content of connective tissue (i.e. desmoplasia) in these tumors in vivo (Supplemental Fig. S7B,C). Thus, the tumor architecture might, in analogy with applying antibodies [35] and chemical anti-tumor agents [36] and as indicated by previous reports [37-39], represent a physical barrier for CTL infiltration. The in vitro and in vivo models presented in this study might help to further verify this hypothesis and to identify specific molecules in the extracellular matrix of tumors accessible for therapeutic intervention to reduce this CTL barrier. Since desmoplasia in man correlates with the progression of solid tumors [40], our data suggest that there are at least two interrelated factors associated with a high tumor load hampering the success of allogeneic immunotherapy, namely the unfavorable in vivo effector to target cell ratio and the tumor composition. These data may partially explain the experience after allogeneic SCT for leukemia [7,41] and solid tumor [42] treatment, that allo-immunotherapeutic effects are generally most successful in minimal residual disease. Thus, optimally, tumor reduction by e.g. surgery, chemo- or radiotherapy should precede a consolidation with allogeneic SCT combined with tumor mHag specific immunotherapy.

Evidently, T-cell depletion with subsequent infusion of only tumor mHag specific CTLs is the safest form of exploiting tumor mHag mismatches between donor and patient. However, murine studies suggest that GvHD provides an optimal pro-inflammatory environment for the efficacy of CTLs directed against tumor-restricted antigens [43]. Of course, questions regarding the interplay between GvHD and GvT effects cannot be addressed in our in vivo models, because of the absence of human GvHD target antigens in NOD/scid mice. Ongoing and future clinical studies will show whether tumor mHag CTLs are most effective during mild and manageable GvHD, thus favoring non-T-cell depleted allogeneic SCT or donor lymphocyte infusions as platform for tumor mHag specific immunotherapy of solid tumors [7].

Conclusion

We have shown the first proof of concept that tumor mHag CTLs can induce strong effects against metastatic cancer in vivo. Thus, mismatched mHags with hematopoiesis- and solid tumor-restricted expression are excellent tools to boost the allo-immune response against solid tumors after HLA-matched allogeneic SCT. These findings pave the way towards allo-immunotherapy protocols for metastatic cancer that do not risk severe GvHD and which overcome – due to the "allo-ness" of the mHag target molecules – the major limitation of current immunotherapies in the autologous setting, namely self-tolerance. A novel approach for enhancing the allo-immune response against tumor mHags is mHag peptide vaccination. Tumor mHag CTLs "naturally" arising after HLA-matched allogeneic SCT may be boosted by repetitive administration of the patient's mHag peptides – an approach we are currently testing in a first phase I/II study for patients with renal cell carcinoma.

ACKNOWLEDGEMENTS

This work was supported by the Dutch Cancer Society (Koningin Wilhelmina Fonds, project code UL2006-3482), the German Research Foundation (Deutsche Forschungsgemeinschaft, fellowship HA-3320/1-1) and the Netherlands organization for Scientific Research (NWO). The authors thank Mr. Jos Pool for excellent technical assistance, Dr. Benoit Van den Eynde and Dr. Peter Schrier for providing important cell lines, Dr. Martin Stern, Dr. Yvette Hensbergen and Dr. Attilio Bondanza for fruitful discussions and Prof. Anneke Brand, Prof. Kees Melief and Dr. Marieke Hoeve for critical reading of the manuscript.

REFERENCES

(1) Eibl B, Schwaighofer H, Nachbaur D et al. Evidence for a graft-versus-tumor effect in a patient treated with marrow ablative chemotherapy and allogeneic bone marrow transplantation for breast cancer. Blood. 1996;88:1501-1508.

(2) Ueno N, Rondon G, Mirza N et al. Allogeneic peripheral-blood progenitor-cell transplantation for poor-risk patients with metastatic breast cancer. J. Clin. Oncol. 1998;16:986-993.

(3) Childs R, Chernoff A, Contentin N et al. Regression of metastatic renal-cell carcinoma after nonmyeloablative allogeneic peripheral-blood stem-cell transplantation. N. Engl. J. Med. 2000;343:750-758.

(4) Bregni M, Dodero A, Peccatori J et al. Nonmyeloablative conditioning followed by hematopoietic cell allografting and donor lymphocyte infusions for patients with metastatic renal and breast cancer. Blood. 2002;99:4234-4236.

(5) Bishop M, Fowler D, Marchigiani D et al. Allogeneic lymphocytes induce tumor regression of advanced metastatic breast cancer. J. Clin. Oncol. 2004;22:3886-3892.

(6) Carella AM, Beltrami G, Corsetti MT et al. Reduced intensity conditioning for allograft after cytoreductive autograft in metastatic breast cancer. Lancet. 2005;366:318-320.

(7) Hambach L, Goulmy E. Immunotherapy of cancer through targeting of minor histocompatibility antigens. Curr. Opin. Immunol. 2005;17:202-210.

(8) Goulmy E. Human minor histocompatibility antigens. Curr. Opin. Immunol. 1996;8:81.

(9) Mapara M, Sykes K. Tolerance and cancer: mechanisms of tumor evasion and strategies for breaking tolerance. J. Clin. Oncol. 2004;22:1136-1151.

(10) de Bueger M, Bakker A, van Rood J, van der Woude F, Goulmy E. Tissue distribution of human minor histocompatibility antigens. Ubiquitous versus restricted tissue distribution indicated heterogenity among human cytotoxic T lymphocyte-defined non-MHC antigens. J. Immunol. 1992;149 (5):1788-1794.

(11) Dickinson A, Wang X, Sviland L et al. In situ dissection of the graft-versus-host activities of cytotoxic T cells specific for minor histocompatibility antigens. Nat. Med. 2002;8:410-414.

(12) Klein C, Wilke M, Pool J et al. The hematopoietic system-specific minor histocompatibility antigen HA-1 shows aberrant expression in epithelial cancer cells. J. Exp. Med. 2002;196:359-368.

(13) Fuji N, Hiraki A, Ikeda K et al. Expression of minor histocompatibility antigen, HA-1, in solid tumor cells. Transplantation. 2002;73:1137-1141.

(14) Akatsuka Y, Nishida T, Kondo E et al. Identification of a polymorphic gene, BCL2A1, encoding two novel hematopoietic lineage-specific minor histocompatibility antigens. J. Exp. Med. 2003;197:1489-1500.

(15) Spierings E, Drabbels J, Hendriks M et al. A uniform genomic minor histocompatibility antigen typing methodology and database designed to facilitate clinical applications. PLoS ONE. 2006;1:e42.

(16) Mutis T, Verdijk R, Schrama E et al. Feasibility of immunotherapy of relapsed leukemia with ex vivo-generated cytotoxic T lymphocytes specific for hematopoietic system-restricted minor histocompatibility antigens. Blood. 1999;93:2336-2341.

(17) Spierings E, Vermeulen C, Vogt M et al. Identification of HLA class II-restricted H-Y specific T helper epitope evoking CD4+ T-helper cells in H-Y-mismatched transplantation. Lancet. 2003;362:590-591.

(18) Wei W, Miller B, Gutierrez R. Inhibition of tumor growth by peptide specific cytotoxic T lymphocytes in a three-dimensional collagen matrix. J. Immunol. Methods. 1997;200:47-54.

(19) Nijmeijer B, Willemze R, Falkenburg J. An animal model for human cellular immunotherapy: specific eradication of human acute lymphoblastic leukemia by cytotoxic T lymphocytes. Blood. 2002;100:654-660.

(20) Hambach L, Nijmeijer B, Aghai Z et al. Human cytotoxic T lymphocytes specific for a single minor histocompatibility antigen HA-1 are effective against human lymphoblastic leukaemia in NOD/scid mice. Leukemia. 2006;20:371-374.

(21) Price JE, Polyzos A, Zhang RD, Daniels LM. Tumorigenicity and metastasis of human breast carcinoma cell lines in nude mice. Cancer Res. 1990;50:717-721.

(22) Tykodi S, Warren E, Thompson J et al. Allogeneic hematopoietic cell transplantation for metastatic renal cell carcinoma after nonmyeloablative conditioning: toxicity, clinical response, and immunological response to minor histocompatibility antigens. Clin. Cancer Res. 2004;10:7799-7811.

(23) Dangles-Marie V, Richon S, El Behi M et al. A three-dimensional tumor cell defect in activating autologous CTLs is associated with inefficient antigen presentation correlated with heat shock protein-70 down regulation. Cancer Res. 2003;63:3682-3687.

(24) Feder-Mengus C, Ghosh S, Weber WP et al. Multiple mechanisms underlie defective recognition of melanoma cells cultured in three-dimensional architectures by antigen-specific cytotoxic T lymphocytes. Br. J. Cancer. 2007;96:1072-1082.

(25) Sutherland R. Cell and environment interactions in tumor microregions: the multicell spheroid model. Science. 1988;240:177-184.

(26) Desoize B, Jardillier J. Multicellular resistance: a paradigm for clinical resistance? Crit. Rev. Oncol. Hematol. 2000;36:193-207.

(27) de Vries TJ, Smeets M, de Graaf R et al. Expression of gp100, MART-1, tyrosinase, and S100 in paraffin-embedded primary melanomas and locoregional, lymph node, and visceral metastases: implications for diagnosis and immunotherapy. A study conducted by the EORTC Melanoma Cooperative Group. J. Pathol. 2001;193:13-20.

(28) Jungbluth AA, Stockert E, Chen YT et al. Monoclonal antibody MA454 reveals a heterogeneous expression pattern of MAGE-1 antigen in formalin-fixed paraffin embedded lung tumours. Br. J. Cancer. 2000;83:493-497.

(29) Jungbluth AA, Chen YT, Stockert E et al. Immunohistochemical analysis of NY-ESO-1 antigen expression in normal and malignant human tissues. Int. J. Cancer. 2001;92:856-860.

(30) Meunier MC, Delisle JS, Bergeron J et al. T cells targeted against a single minor histocompatibility antigen can cure solid tumors. Nat. Med. 2005;11:1222-1229.

(31) Meidenbauer N, Marienhagen J, Laumer M et al. Survival and tumor localisation of adoptively transferred melan-A specific T cells in melanoma patients. J. Immunol. 2003;170:2161-2169.

(32) Vignard V, Lemercier B, Lim A et al. Adoptive transfer of tumor-reactive Melan-A-specific CTL clones in melanoma patients is followed by increased frequencies of additional Melan-A-specific T cells. J. Immunol. 2005;175:4797-4805.

(33) Yee C, Thompson JA, Byrd D et al. Adoptive T cell therapy using antigen-specific CD8+ T cell clones for the treatment of patients with metastatic melanoma: in vivo persistence, migration, and antitumor effect of transferred T cells. Proc. Natl. Acad. Sci. U.S.A. 2002;99:16168-16173.

(34) Zhang B, Bowerman NA, Salama JK et al. Induced sensitization of tumor stroma leads to eradication of established cancer by T cells. J. Exp. Med. 2007;204:49-55.

(35) Netti PA, Berk DA, Swartz MA, Grodzinsky AJ, Jain RK. Role of extracellular matrix assembly in interstitial transport in solid tumors. Cancer Res. 2000;60:2497-2503.

(36) Minchinton AI, Tannock IF. Drug penetration in solid tumours. Nat. Rev. Cancer. 2006;6:583-592.

(37) Yang Q, Goding S, Hagenaars M et al. Morphological appearance, content of extracellular matrix and vascular density of lung metastases predicts permissiveness to infiltration by adoptively transferred natural killer and T cells. Cancer Immunol. Immunother. 2006;55:699-707.

(38) Kuppen PJ, van der Eb MM, Jonges LE et al. Tumor structure and extracellular matrix as a possible barrier for therapeutic approaches using immune cells or adenoviruses in colorectal cancer. Histochem. Cell Biol. 2001;115:67-72.

(39) Singh S, Ross SR, Acena M, Rowley DA, Schreiber H. Stroma is critical for preventing or permitting immunological destruction of antigenic cancer cells. J. Exp. Med. 1992;175:139-146.

(40) Kaariainen E, Nummela P, Soikkeli J et al. Switch to an invasive growth phase in melanoma is associated with tenascin-C, fibronectin, and procollagen-I forming specific channel structures for invasion. J. Pathol. 2006;210:181-191.

(41) Barrett A. Allogeneic stem cell transplantation for chronic myeloid leukemia. Semin Hematol. 2004;40:59-71.

(42) Carella AM, Bregni M. Current role of allogeneic stem cell transplantation in breast cancer. Ann Oncol. 2007;18:1591-1593.

(43) Stelljes M, Strothotte R, Pauels H et al. Graft-versus-host disease after allogeneic hematopoietic stem cell transplantation induces a CD8+ T cell-mediated graft-versus-tumor effect that is independent of the recognition of alloantigenic tumor targets. Blood. 2004;104:1210-1216.

SUPPLEMENTARY TABLES AND FIGURES

Tumor cell line	HA-1 genomic typing	HA-1 mRNA	H-Y genomic typing	Histology of the primary malignancy	Reference
BB65-RCC	H/R	+	+	primary kidney tumor with clear cell carcinoma histology, grade II to III	B. Van den Eynde (personal communication)
MDA-MB 231	H/R	+	-	Pleural effusion of poorly differentiated mammary adenocarcinoma	1
518A2	H/R	-	+	metastatic melanoma	2
MCF-7	R/R	-	-	Pleural effusion of mammary adenocarcinoma with ductal structures	3

Table S1. Characteristics of the tumor cell lines used in this study. The tumor cell lines show a differential pattern of the immunogeneic HA-1H allele, the non-immunogeneic HA-1R allele and the mHag H-Y on genomic level and of HA-1 mRNA expression. The tumor cell lines are derived from solid tumors of different entities.

(1) Cailleau R, Young R, Olive M, Reeves WJ, Jr. Breast tumor cell lines from pleural effusions. J Natl Cancer Inst. 1974;53:661-674.
(2) Versteeg R, Noordermeer IA, Kruse-Wolters M, Ruiter DJ, Schrier PI. c-myc down-regulates class I HLA expression in human melanomas. EMBO J. 1988;7:1023-1029.
(3) Soule HD, Vazguez J, Long A, Albert S, Brennan M. A human cell line from a pleural effusion derived froma breast carcinoma. J Natl Cancer Inst. 1973;51:1409-1416.

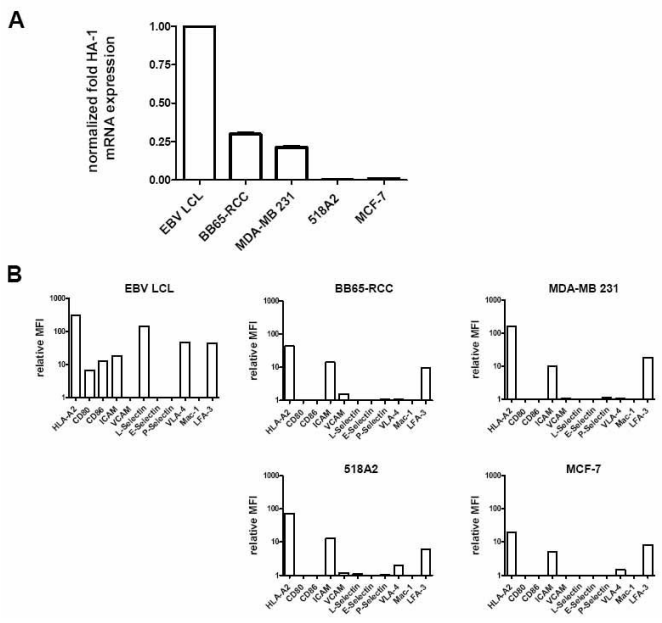

Figure S1. Expression of HA-1 mRNA and cell surface molecules in the tumor cell lines. (A) HA-1 mRNA expression levels in different tumor cell lines. Depicted are the relative levels of HA-1 mRNA expression in different tumor cell lines using EBV LCLs as reference determined by quantitative PCR. Results were normalized with 18S mRNA. (B) Expression of cell surface molecules in different tumor cell lines and EBV LCLs determined by flowcytometry. X-axis: HLA-A2, the co-stimulatory molecules CD80 and CD86 and the cell adhesion molecules ICAM and VCAM, L-, E and P-Selectin, VLA-4, Mac-1 and LFA-3. Y-axis: mean fluorescence intensity (MFI) in relation to the isotype control.

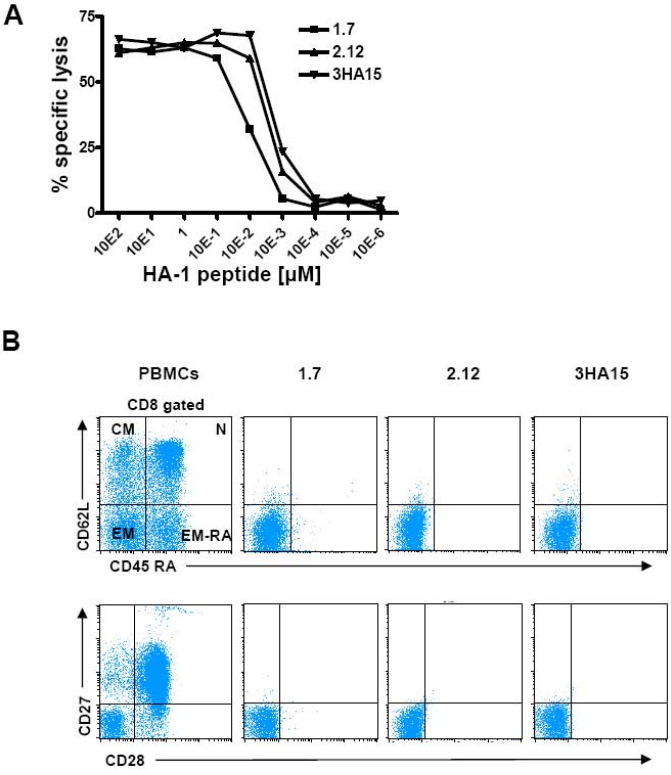

Figure S2. Detailed characterization of the human HA-1 CTL clones. (A) Response of HA-1 specific CTL clones to serial dilutions of HA-1 peptide loaded on EBV LCLs in a Cr51 release assay. (B) HA-1 CTL clones were analyzed for the markers CD45RA and CD62L in order to categorize them as naïve (N), central memory (CM), effector memory (EM) or EM-RA cells. Subsequently, HA-1 CTL clones were stained for CD27 and CD28 to determine the differentiation stage of the CTLs. PBMCs are shown as controls.

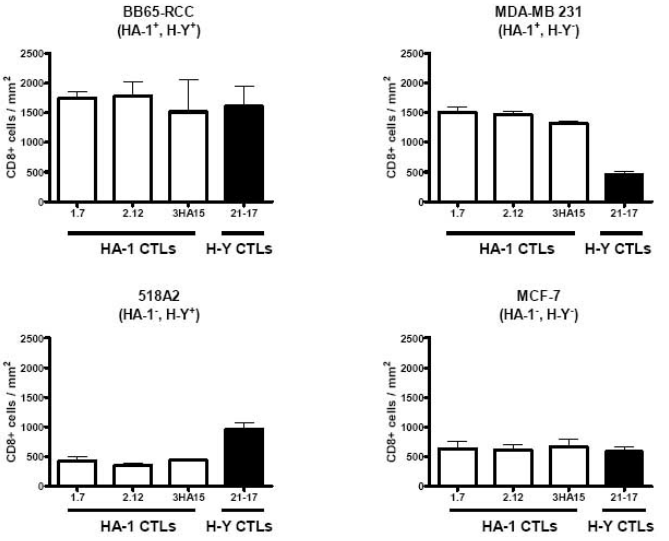

Figure S3. Infiltration of microtumors by different CTL clones. Microtumors were co-incubated with different HA-1 CTLs and H-Y CTLs for 3 days in an effector-target ration of 15:1 and tumor infiltration by CTLs was determined by immunohistochemistry for CD8. X-axis: the HA-1 CTL clones 1.7, 2.12 and 3HA15 and the H-Y CTL clone 21-17; Y-axis: number of CD8 + staining cells / mm2 on median 7 parallel sections (3-13) per CTL clone.

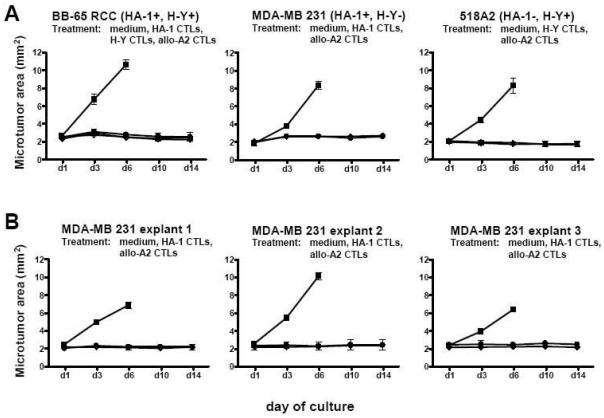

Figure S4. Long-term monitoring of microtumor growth after CTL treatment. Microtumors were generated from (A) tumor cell lines from in vitro culture or (B) MDA-MB 231 cells explanted from s.c. tumors grown in NOD/scid mice for 4 weeks. Each line represents mean microtumor area +/- SEM (median 3 (range 3-5) microtumors per condition). X-axis: day of culture; y-axis: microtumor area (mm2). Treatment: HA-1 CTLs (E:T ratio 15:1) ♦; H-Y CTLs (E:T ratio 15:1) ◊; allo-HLA-A2 CTLs (E:T ration 15:1) ●; medium ■. Tumor growth in the medium control wells was terminated on day 6 due to beginning overgrowth of the culture well.

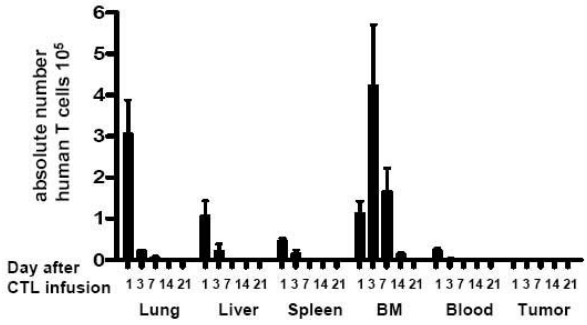

Figure S5. In vivo distribution of HA-1 CTLs. NOD/scid mice with s.c. MDA-MB 231 macrotumors received i.v. a single dose of 30x106 HA-1 CTLs (clone 1.7). HA-1 CTLs were quantified in lung, liver, spleen, bone marrow, peripheral blood and the solid tumor at 1, 3, 7, 14 or 21 days after CTL transfer. Depicted are the absolute numbers of viable human CTLs in the individual tissues. Bars correspond to mean +/- S.E.M. (4 mice per measurement time point).

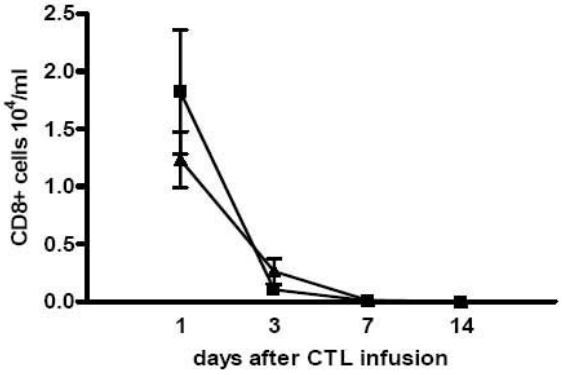

Figure S6. Kinetic of CTLs in the peripheral blood in the pulmonary microtumor model. On the X-axis is depicted the time after HA-1 or H-Y CTL inoculation. On the Y-axis is depicted the mean CD8 cell counts +/- SEM in the peripheral blood of mice (6 mice per group). Treatment: closed squares: HA-1 CTL clone; triangles: H-Y CTLs.

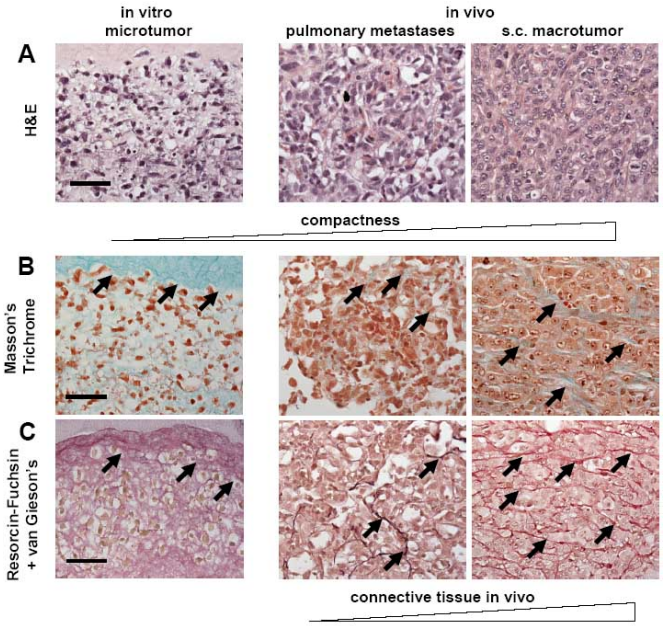

Figure S7. Connective tissue in MDA MB-231 tumors grown in vitro and in vivo. In vitro microtumors, pulmonary metastases and s.c. tumors were stained with H&E (A) and with the connective tissue stains Masson's Trichrome (B) and Resorcin-Fuchsin counterstained with van Gieson's (C). (B) Masson's Trichrome: collagen – green, cytoplasm – red, nuclei – dark brown; arrowheads: collagen (green). (C) Resorcin-Fuchsin counterstained with van Gieson's: elastic fibres - black, collagen – red, cytoplasm – yellow/brown, nuclei –brown; arrowheads: micro- and macrotumor: collagen (red), pulmonary metastases: elastic fibres (black); bar, 100 µm.